Myoelectric control with abstract decoders

Myoelectric control with abstract decoders

OPEN ACCESS
IOP Publishing
Journal of Neural Engineering
J. Neural Eng. **15** (2018) 056003 (15pp)
https://doi.org/10.1088/1741-2552/aacbfe

Myoelectric control with abstract decoders

Matthew Dyson[1], **Jessica Barnes**[1] **and Kianoush Nazarpour**[1,2]

[1] Intelligent Sensing Laboratory, School of Engineering, Newcastle University, NE1 7RU, United Kingdom
[2] Institute of Neuroscience, Newcastle University, Newcastle-upon-Tyne, NE2 4HH, United Kingdom

E-mail: Matthew.Dyson@newcastle.ac.uk and Kianoush.Nazarpour@newcastle.ac.uk

Received 15 November 2017, revised 4 June 2018
Accepted for publication 12 June 2018
Published 2 July 2018

Abstract

Objective. The objective of this study was to compare the use of muscles appropriate for partial-hand prostheses with those typically used for complete hand devices and to determine whether differences in their underlying neural substrates translate to different levels of myoelectric control. *Approach.* We developed a novel abstract myoelectric decoder based on motor learning. Three muscle pairs, namely, an intrinsic and independent, an intrinsic and synergist and finally, an extrinsic and antagonist, were tested during abstract myoelectric control. Feedback conditions probed the roles of feed-forward and feedback mechanisms. *Results.* Both performance levels and rates of improvement were significantly higher for intrinsic hand muscles relative to muscles of the forearm. Intrinsic hand muscles showed considerable improvement generalising to decoder use without visual feedback. Results indicate that visual feedback from the decoder is used for transitioning between muscle activity levels, but not for maintaining state. Both individual and group performance were found to be strongly related to motor variability. *Significance.* Physiological differences inherent to the hand muscles can translate to improved prosthesis control. Our results support the use of motor learning based techniques for upper-limb myoelectric control and strongly argues for their utility in control of partial-hand prostheses. We provide evidence of myoelectric control skill acquisition and offer a formal definition for abstract decoding in the context of prosthetic control.

Keywords: abstract decoding, electromyography, motor learning, upper-limb prosthesis

Supplementary material for this article is available online

(Some figures may appear in colour only in the online journal)

1. Introduction

Myoelectric control refers to the use of the electromyogram (EMG) as a control signal for powered limb prostheses. Estimating intent from residual muscle activity can provide a non-invasive communication channel between the nervous system and an artificial limb. Myoelectric control has attractive properties: the physical effort required resembles that of existing limbs, sensor systems are compact and the EMG signal can readily be adapted to proportional control [1].

The conventional 'dual-site' approach for prosthesis control usually uses the EMG signals from two residual muscles to provide bidirectional control of one degree of freedom (DoF), or more, after invasive surgery [2–4]. As such, it has been widely utilised for myoelectric hand control in people with trans-radial limb difference, for whom only muscles of the forearm remain.

Current generation myoelectric hand prostheses offer multiple DoFs. This technology now extends to digit prostheses for people with partial-hand loss [5]. An example commercial product is the i-digits™ quantum prosthesis (Touch Bionics, UK). Considering amputation statistics, the growth of the partial-hand prosthesis market is not surprising. Over 90% of upper-limb amputations in the US are to the fingers or hands

[6]. In the UK, partial-hand and digit loss comprise approximately 39% of referrals to prosthetic clinics [7]. Partial-hand amputees perceive their loss as disproportionately affecting work and may face problems returning to, and retaining, employment [8, 9].

Partial-hand prostheses bring new design specifications and constraints. Myoelectric control strategies must be selected based on the available intrinsic myoelectric sites (located in the hand) and, where possible, the functional range of the wrist should be preserved [10–12]. While modern digit prostheses offer multiple DoFs the current clinical standard for partial-hand prosthesis control is conventional amplitude-based, dual-site control. However, there are fundamental differences between the neural substrates controlling muscles of the forearm and intrinsic hand muscles [13]. For instance, fractionation of muscle activity in the hand is enhanced by the corticomotoneuronal pathways [13, 14]. Hand muscles have higher proportions of beta-innervated muscle spindles and lack both reciprocal inhibition between antagonist muscles and recurrent motoneurone axon collaterals [13]. These neural substrates, despite the existence of common corticospinal input to spinal motorneuron pools, allow almost-independent *neural* control of intrinsic hand muscles. Indeed, the anatomical structure of the hand limits finger independence to a greater degree than the neuromotor system [15].

A drive toward simultaneous and proportional multifunctional control means muscle synergies will play a fundamental role in future myoelectric decoders [16]. However, the degree to which this type of muscle activity can be modified to optimise control is a current topic of debate. de Rugy *et al* [17] tested biomechanically-dependent muscles in the forearm and concluded that muscle synergies reflect learned, locally optimal, control strategies which, having become habitual within a hierarchical system, are relatively inflexible to alteration. Nazarpour *et al* [18] tested biomechanically-independent and antagonistic muscle pairs during the operation of a myoelectric task and found participants developed task-dependent muscle synergies flexibly via the interaction of feed-forward and feedback mechanisms. Similarly, Ison and Artemiadis [19] found synergies emerged in biomechanically-independent antagonist muscle pairs as participants identified and adapted to system dynamics during multi-day use of a closed-loop motor learning-based decoder.

In this work, we study the use of muscles appropriate for partial-hand prostheses with those typically used for complete hand devices during use of an 'abstract decoder', a motor learning-based method currently generating interest as an alternative approach to myoelectric prosthesis control [19–24]. Our comparison is motivated by the assumption that almost-independent *neural* control of intrinsic hand muscles is advantageous in a motor learning context. This position is supported by previous research suggesting that the distal motor system is particularly suited to learning the type of novel neuromotor associations involved in abstract decoding [20]. We therefore compared two pairs of intrinsic hand muscles, an independent pair and a natural synergist, with an extrinsic antagonist pair of forearm muscles while learning to use the decoder. Multiple visual conditions were used to distinguish the roles of feed-forward and feedback mechanisms in developing control. We provide evidence of motor skill acquisition and discuss the implications of our results. Before presenting our analysis we continue with a formal definition of abstract decoding to provide a clear context for our work.

1.1. Abstract decoding

In myoelectric control, the primary alternative to the dual site approach is pattern recognition [4]. While pattern recognition has origins in the numerical sciences, the proposed abstract decoding framework has roots in the neural sciences. We define abstract decoders as '*non-biomimetic decoders reliant upon the closed-loop generation of novel inverse models*'. The following sections provide an outline of how abstract decoders relate to current prosthetic decoding techniques, as outlined in figure 1(a).

1.1.1. Adaptation of inverse models. In motor control, the term 'inverse model' refers to internal models which, given a desired change in state, provide the motor commands required to reach said state [25]. In the context of myoelectric prosthetics, the supervised learning used in approaches such as pattern recognition utilise pre-existing inverse models; that is to say users provide examples of the motor activity they would perform to position a limb in a state, and a relatively static relationship is assumed to exist between motor activities and limb states.

Motor learning based myoelectric-computer interfaces (MCI) exploit the fact that the motor system is able to learn multiple, novel inverse maps to relate motor outputs to arbitrary control variables [25, 26]. To facilitate this learning, motor learning based MCIs present continuous visual feedback of motor activity [27] in a non-representational multidimensional control space, such as cursor control in a center-out task, and the motor system adapts and updates according to the feedback received [28, 29]. An outline of the center-out task used in Pistohl *et al* [21] is shown in figure 1(b). The manner in which control spaces are explored suggests that the process of generating an inverse map is fundamental to this form of learning [26, 30].

This type of closed-loop learning can be used to modify existing muscle behaviour [20] and shows promise for effective post-stroke rehabilitation [31]. Because abstract decoding is the application of an existing approach to neuromotor prosthetics, it inherits a robust theoretical base, which goes some way toward explaining why the approach is quickly gaining traction as a viable prosthesis control technique [19–24, 32, 33]. While this work argues that abstract decoding is a *particularly* suitable control technique for partial-hand prostheses, previous research shows that the approach can also be applied in the more general case of trans-radial limb loss [24, 33].

1.1.2. Estimation of motor commands. Systems that attempt to decode motor commands typically do so to map their estimated output onto a prosthetic state, such that intended movements are used to initiate their prosthetic substitutes. This type of decoding is described as 'biomimetic' and is considered to be intuitive because it limits the cognitive demand placed upon users. One method of implementing intuitive biomimetic

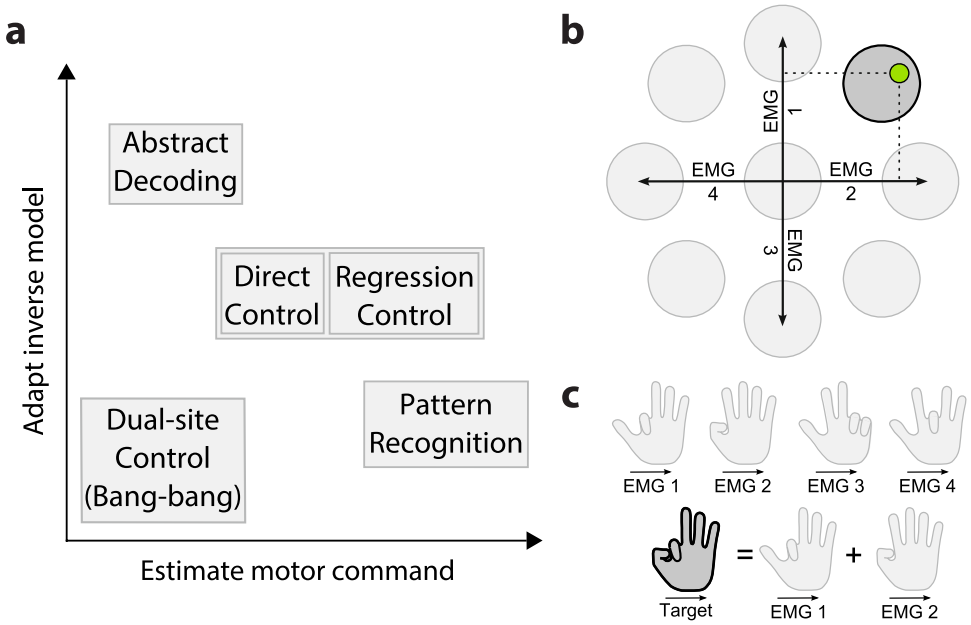

Figure 1. Abstract decoding. (a) High level overview of current prosthetic decoding techniques according to how they typically interact with the motor control system. Control gains may be made either by refining the estimate of the motor command or by inducing changes to the inverse model. (b) An abstract decoding cursor control space based on four EMG channels arranged in a centre-out task, as used in Pistohl *et al* [21]. Circles outline targets, cursor is shown in green, dashed lines indicate EMG activity. (c) Parallel hand posture space mapping used in Pistohl *et al* [21], EMG 1 to 4 show postures corresponding to EMG vectors, target shows the posture corresponding to the control space target in the figure above.

decoding is to estimate the relevant motor commands to individual DoF. This approach has been used in hand prostheses by combining surface EMG with pattern recognition [34], regression [33, 35–38], and by use of intramuscular recording methods [39–41]—denoted 'direct control' in figure 1(a). A more common approach is to estimate an ensemble of motor commands by weighting multiple inputs via pattern recognition [42, 43].

Rather than estimating existing motor commands it is possible to encode behaviour in alternative patterns of neural or muscular activity [44–48]. Alternative patterns are non-biomimetic and therefore non-intuitive, as such they must be learned. Patterns may be learned at the neural or muscular level [20, 49] and understanding how the motor cortex re-purposes normal behaviour to support this type of adaptation is a current area of research [47, 50–52]. Once patterns are learned arbitrary functional outputs may be mapped to the non-representational control space, such as proportional control of prosthetic digits [21] or selection of hand postures [24]. The relationship between functional outputs and cursor position described by Pistohl *et al* [21] is shown in figure 1(c). Because abstract decoders generate new inverse models, or heavily adapt existing ones, control within non-representational space may exhibit intuitiveness [22] but is not biomimetic in the classic sense.

2. Method

2.1. Participants

Twenty five participants took part in this experiment (17 male and 8 female, age: 26 ± 4). All were able-bodied, right-handed and free from neurological or motor disorder. Approval was granted by the local ethics committee at Newcastle University. All participants gave informed written consent. Data collection for one participant was halted early due to lack of attention. A replacement participant was recruited to bring the total number of participants to 24.

2.2. Experimental setup

2.2.1. Recordings. Participants sat in an experimental chair with their right hand restrained in a pronated open position within a modified glove. The fingers and palm of the glove were fixed to a horizontal board which was attached to the armrest of the chair. The position of the board was adjustable to provide comfortable support for each participant's arm and hand. A 17" LCD flat panel display (Belinea 101727, Germany) was positioned approximately 1 m in front of the participant to present visual feedback.

The surface EMG signals were recorded from three intrinsic hand muscles, namely, abductor pollicis brevis (APB); abductor digiti minimi (ADM); and first dorsal interossei (1DI) and two forearm muscles: flexor carpi radialis (FCR) and extensor carpi radialis (ECR). Measurements were made with disposable snap electrodes (Bio-logic®, Natus Medical Inc, USA). Signals were amplified with a gain of 5 K (D360, Digitimer, UK) and band-pass filtered (30 Hz–1 KHz). Signals were sampled at a 5 KHz rate using a data acquisition card (NI USB-6212 BNC, National Instruments, USA). All subsequent computation necessary to realise the experiment were performed on a desktop computer (3.2 GHz i5-3470 CPU, 8 GB RAM, Viglen Ltd, UK) using software developed in Python (Python Software Foundation, USA).

All EMG data were visually inspected for artefacts. Data from trials containing significant movement artefacts, electrical noise or any other signs of non-physiological external influence, were rejected. Mean artefact rejection rate per subject was 0.56% with a standard deviation of 0.8%.

2.2.2. Estimation of muscle activity. Muscle activity was estimated using a mean absolute value (MAV) filter. For each channel, a control signal was calculated by averaging the rectified EMG signal over the preceding 750 ms window. The control signals were updated at a variable rate which exceeded, and was asynchronous to, the rate at which the display was updated. This ensured any changes in EMG activation were perceived to be reflected in the shortest possible time frame. Following [21], the selected window size balanced the requirement for responsive effector movement against that of sufficiently smooth output during constant muscle contraction.

2.2.3. MCI calibration. Prior to each experiment a calibration routine was performed on MAV filtered EMG data. Instructions were given as to the movements required to induce activity in each of the five recording sites. Participants were requested to relax their arm and hand while data representative of baseline resting EMG, y_r, was collected. To determine comfortable contraction levels, y_c, participants were instructed to contract muscles in a manner that could be comfortably maintained and repeated several hundred times without fatigue. Data representative of baseline resting and of comfortable contraction were concatenated and MAV filtered. Calibration levels for each channel, y_r and y_c, were set to the minimum and maximum values of the MAV filtered calibration data. In previous studies with similar myoelectric interfaces, this corresponded to an activity level between 10%–20% of the maximum voluntary contraction [18, 23, 53, 54]. Experiments utilised a normalized muscle activation level, $\check{y}$, which was obtained from muscle activation level, y, the output of the MAV filter applied to raw EMG measurements, according to:

$$\check{y} = (y - y_r)/(y_c - y_r). \quad (1)$$

Estimates of measurement offset values were derived from the calibration data for each EMG channel and applied to experimental data.

2.3. Experimental protocol

Participants used near-isometric muscle contractions to operate the MCI task. The activity of a pair of muscles determined the position of a 2-D cursor within the MCI control space, as outlined in figure 2(a). The control space was a 2-D graph representing normalized muscle activation, $\check{y}$, from two EMG measurements. Cursor position reflected the instantaneous normalized muscle activation level in two EMG measurements, as indicated by the dashed lines in figure 2(a). For clarity, only one of two target layouts is presented in figure 2(a). The target layouts constituted different experimental conditions. The structure of the second layout and its effect on results is presented in supplementary materials (figure S1) (stacks.iop.org/JNE/15/056003/mmedia). The

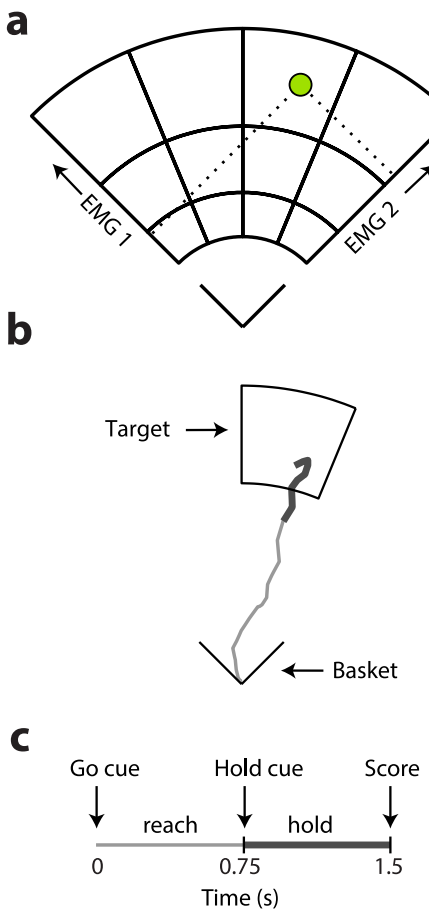

Figure 2. The MCI task. (a) The 2-dimensional myoelectric interface control space. Participants use co-contraction of a muscle pair to move the virtual cursor toward a target. Dashed lines represent the magnitude of activation in the two EMG channels. (b) A representative cursor trajectory in the task space. Thin and thick traces show trajectories during reach and hold periods respectively. (c) Task timing structure denoting cues, reach and hold periods.

interface was calibrated such that: a comfortable muscle contraction, normalized muscle activation $\check{y} \approx 1$, would bring the cursor to the upper limit of the interface; a third of this level of activity, $\check{y} \approx 0.3$, defined the lower bounds of the targets; and approximately a fifth of a comfortable contraction level, $\check{y} \approx 0.2$, defined the upper edge of the basket below the target space.

Figure 2(b) shows a representative cursor trajectory for an individual trial. At the start of a trial the cursor and the basket at the base of the interface were presented. If the participant was not in a suitably relaxed state at this time trial updates would pause and the basket was highlighted. Once the participant retained the cursor within the basket for 250 ms the trial would continue. One of the twelve targets shown in figure 2(a) was then presented and the standard trial phases (figure 2(c)) began.

Each trial was 1.5 s long and composed of two 750 ms periods: 'reach' and 'hold', as outlined in figure 2(c). The first 750 ms, the reach period, was allocated for moving the cursor from the basket to the target. During the second 750 ms, the hold period, participants were instructed to retain the cursor within the target area. A 'hold score' was calculated, measuring the degree to which the target was within, or in contact with, the

target during the hold period. At trial completion the hold score was presented to the participant for 1 s. After that, a 2 s inter-trial interval followed, during which the screen was blanked. Participants did not see the cursor traces shown in figure 2(b).

2.3.1. Muscle groups. Our objective was to compare the performance of muscles appropriate for partial-hand prosthesis with those used for complete hand devices. We tested intrinsic muscles accessible from the palmar or lateral side of the hand. The thenar and hypothenar eminences are the most logical control sites in the case of full digit loss because of the size of the muscles and their separability [10]. The thenar and hypothenar are represented in our first intrinsic pair, that is, APB–ADM. However, the hypothenar compartment can also allow individuals with partial-hand loss to retain touch sensations while using a prosthesis [55]. Our second intrinsic pair, that is, 1DI–APB, allows for touch feedback in the case of full digit loss. The most common pair of muscles used to control complete hand devices are ECR–FCR, this pair was used as our extrinsic muscle pair. The muscles tested as control groups for the proposed MCI, and the movements required to generate activity, were therefore as follow:

- **APB–ADM**: are independent as they do not form a common synergist pair. The movements requested of participants were abduction of the thumb and abduction of the little finger.
- **1DI–APB**: represent an existing synergistic muscle pair. Participants were instructed to perform abduction of the index finger and abduction of the thumb.
- **ECR–FCR**: are an antagonist pair which do not co-contract naturally. Restrained extension and flexion of the wrist were demonstrated as the movements required for EMG activity.

2.3.2. Feedback conditions. Three feedback conditions were utilised during the experiment, each differing with respect to cursor visibility. The feedback conditions used are defined as follows:

- **Full**: The cursor was visible during both the reach and the hold periods.
- **Reach**: The cursor was visible during the reach, but not during the hold period.
- **Zero**: The cursor was not visible during neither the reach nor the hold period.

The two incomplete feedback conditions were intended to probe the degree to which visual feedback was required by participants to guide the cursor. Trials with no visual feedback were intended to measure the degree to which participants had internalised overall task requirements such that they were able to reproduce muscle activations.

2.4. Experiment structure

Prior to each experimental condition, participants were informed as to which pair of muscles to use but were not informed how muscle activations related to cursor movement. A description was provided of the three feedback conditions used in the experiment. Participants were instructed to attempt to reach the target and maximise their overall score, irrespective of the feedback presented. For each muscle pair, participants performed four runs of 72 trials for two target area conditions. The three feedback conditions were pseudo-randomised throughout the 72 trial runs: 48 of 72 trials used the Full feedback condition, 12 trials used the Reach feedback condition and 12 trials were presented with the Zero feedback condition. The order in which muscle pairs and target layouts were tested were counter-balanced across participants to ensure each permutation of experimental conditions was represented by an equal number of participants.

2.5. Further definitions

A number of metrics were used during analysis and are defined here for convenience.

- **Hold score** measures the quality of the dwell within a target. It is defined as the percentage of time that the cursor remains within, or in contact with, the target during the hold period.
- **Hit score** provides information as to the number of targets being reached. It is a binary equivalent of the hold score, a hit score of one indicates a hold score above zero.
- **Overshoots** provide insight into cursor control by measuring the number of times the cursor leaves the target area after having been in contact with it.
- **Reaction time** defines the time elapsing between presentation of the target and the participants response. Reaction time was determined from EMG using a threshold based method introduced by Solnik *et al* [56, 57]. In brief, the EMG signal was conditioned using a discrete Teager Kaiser energy operator (TKEO) to calculate the energy derived from instantaneous signal amplitude and instantaneous signal frequency. Conditioning enhances the signal to noise ratio (SNR) to improve onset detection [58]. Onset was marked where TKEO first exceeded threshold in each trial. Threshold values were manually calibrated post hoc.
- **Path efficiency** describes the optimality of the cursor trajectory by dividing the length of the fastest route to the target over that taken. Path start was defined as cursor position at reaction time. End point was defined as where the optimal route to the target centroid intersected the target bounds.
- **Coefficient of variation** is a measure of EMG signal variability. It is the ratio of the standard deviation of an EMG sample over its mean absolute value. Unless otherwise noted coefficient of variation was calculated over the hold period.

Hold Score was used as the primary performance metric. Hit Score can provide valuable information when participants exhibit low levels of cursor control but does not discriminate between degrees of more nuanced control; and is therefore

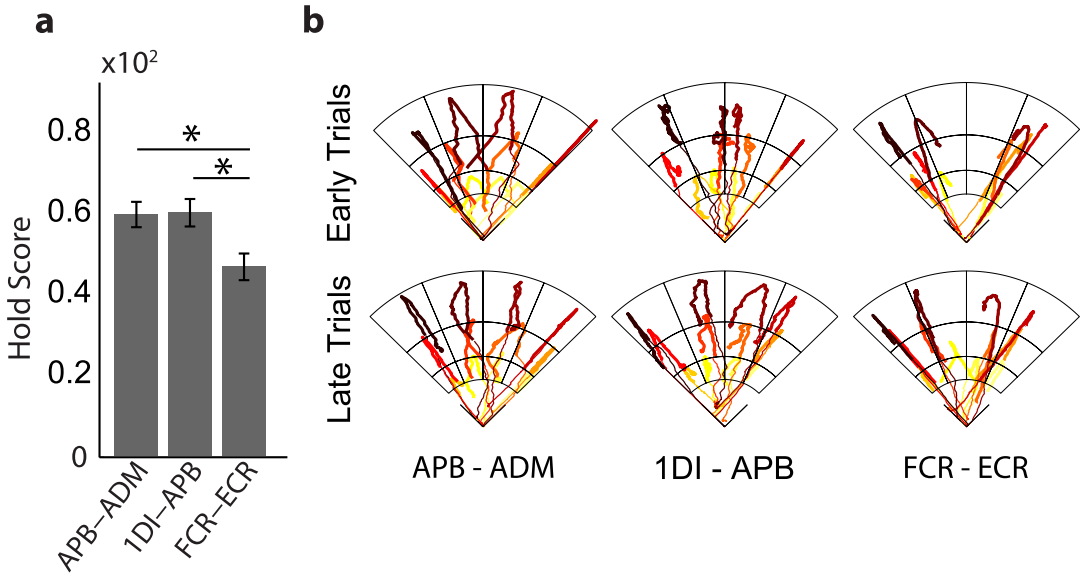

Figure 3. MCI performance. (a) Final run hold score for each muscle group. Asterisks denote significant differences in performance. (b) Sample single trial cursor trajectories from one participant's first and final run. Samples shown for each target and muscle pair. Upper row shows trajectories from the first run. Lower row shows trajectories from the final run. Thicker lines indicate the hold period.

hard to generalise from. In general, Hit Score showed rapid gains in early runs but tended to plateaux on or by the third run, especially in intrinsic muscle pairs, as shown in supplementary materials figure S2.

2.6. Statistics

Hold score performance values were normally distributed within individual muscle pairs. When grouping data according to feedback condition, and pooling muscle pair data, distributions were skewed due to differences in performance. For consistency we use non-parametric statistical measures for comparing across groups, z-statistics are reported when approximate methods are used. Statistical analysis was performed in MATLAB (MathWorks, MA, USA). Comparisons of correlation were performed in the R environment (The R Foundation, Vienna, Austria) using the Cocor toolbox [59].

3. Results

Results are presented in four sub-sections. Performance rates across targets for each muscle group and feedback condition are presented in section 3.1. Section 3.2 provides an overview of how performance improves over runs and to what degree this improvement generalises for each of the muscle pairs tested. Salient differences between the feedback conditions are outlined in section 3.3. Finally, improvement in participant performance is analysed in the context of motor variability and skill acquisition in section 3.4.

3.1. Overall MCI performance

MCI performance across muscle groups was measured by comparing the final experimental runs in each condition. Mean hold score values for each muscle pair, in the Full feedback condition and for the final experimental run, are shown in figure 3(a). In the Full feedback condition, there was a significant difference in performance between APB–ADM ($Mdn = 0.64$) and FCR–ECR ($Mdn = 0.5$) (Wilcoxon Signed-Ranks Test, $Z = 3.49$,$p < 10^{-3}$) and also between 1DI–APB ($Mdn = 0.63$) and FCR–ECR (Wilcoxon Signed-Ranks Test, $Z = 3.77$,$p < 10^{-3}$). There was no significant difference between APB–ADM ($Mdn = 0.64$) and 1DI–APB ($Mdn = 0.63$). Parallel significant differences were found in the Reach feedback condition between APB–ADM ($Mdn = 0.6$) and FCR–ECR ($Mdn = 0.4$) (Wilcoxon Signed-Ranks Test, $Z = 2.97$,$p < 10^{-2}$) and between 1DI–APB ($Mdn = 0.59$) and FCR–ECR ($Mdn = 0.4$) (Wilcoxon Signed-Ranks Test, $Z = 2.91$,$p < 10^{-2}$). These results suggest that intrinsic muscle groups allow for better MCI control than extrinsic muscles.

Single-trial cursor trajectories selected from positively scoring trials for each target from a participant's first and final runs are shown in figure 3(b). The participant commenced control using muscle pair 1DI–APB and followed with FCR–ECR and APB–ADM. Trajectories for the synergist pair, 1DI–APB, travel in directions which are independent of the interface, suggesting *existing* co-contraction behaviour during the initial run. In contrast, trajectories for the independent pair, APB–ADM, often move in parallel to the edges of the interface. These patterns are indicative of serial, rather than parallel, changes in EMG amplitude. For both intrinsic pairs, sample trajectories in the final trial are more direct and hold period activity is generally closer to the target centroids. Note that in the final trials, right edge column target trajectories for the independent pair, APB–ADM, run close to the interface border; in contrast, the corresponding trajectories for the synergist pair, 1DI–APB, are closer to the midline, indicative of undesired muscle co-activation. In early trials trajectories for the extrinsic pair, FCR–ECR, fail to reach the central targets, indicating a lack of coordinated co-contraction. Final run

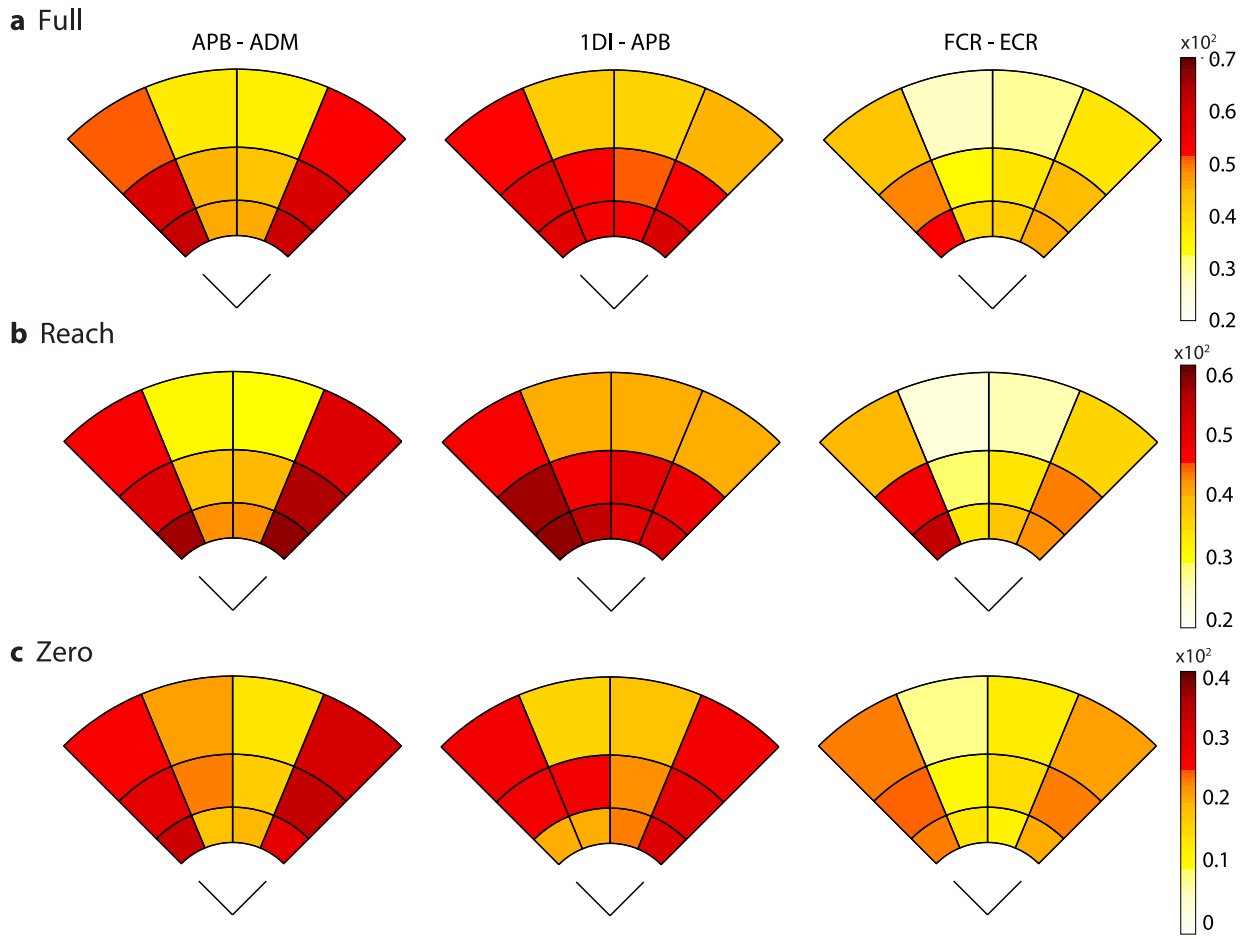

Figure 4. Heat maps detailing hold score for individual targets. Darker colours indicate better performance. Columns left to right show results for muscle pairs APB–ADM, 1DI–APB and FCR–ECR. Feedback conditions are shown on rows: (a) Full; (b) Reach; and (c) Zero. Note: In the interest if clarity in presentation, each row has an independent scale.

trajectories for FCR–ECR show improved co-contraction but performance over central targets does not match that of the intrinsic pairs.

Figure 4 shows heat maps outlining individual target hold scores for each of the muscle pairs and feedback conditions tested across all participants. Significant symmetry may be observed across the mid-line for each muscle pair, with targets on the left and rightward edge generally scoring higher than central targets. Higher scores for edge targets are expected, because moving to these positions only requires the activation of one muscle. This supposition assumes that each muscle in a pair can be activated independently. We measure the degree of similarity of performance across the mid-line of the interface for each muscle pair using Pearson's correlation coefficient. In the Full feedback condition, figure 4(a), this relationship is strongest for APB–ADM ($r = 0.99, n = 6, p < 10^{-3}$) and weaker for FCR–ECR ($r = 0.92, n = 6, p < 10^{-2}$) and 1DI–APB ($r = 0.90, n = 6, p = 0.015$), where n refers to 6 targets each side of the mid-line. Correlation values for the independent pair, APB–ADM, were significantly greater than for the synergist pair, 1DI-APB, (Meng's z-test, $Z = 2.94, p < 10^{-2}$). This difference is attributable to unwanted co-activation preventing optimal performance on right column targets, visible in the Full and Reach conditions in figure 4 and repeating the trajectories shown in figure 3(b).

Equivalent heat maps to those shown in figure 4 can be generated for target hit score. If low hold scores for certain targets result from the targets being missed, rather than an inability to hold within the target, we would expect to observe a relationship between hit and hold scores. Correlation between individual target hit score and individual target hold score ($n = 12$ targets) was highest in the case of APB–ADM ($r = 0.95, n = 12, p < 10^{-4}$), a strong relationship also held for FCR–ECR ($r = 0.83, n = 12, p < 10^{-3}$) while 1DI–APB showed a weaker but significant interaction ($r = 0.64, n = 12, p = 0.025$). Correlation between hold score and hit score was significantly higher for the independent pair, APB–ADM, than the synergist pair, 1DI–APB, (Raghunathan's z-test, $Z = 2.36, p = 0.019$). Low correlation values in the case of 1DI–APB are likely to be attributable to participants having difficulty retaining the cursor in peripheral targets due to unwanted co-activation.

If reducing visual feedback impacts upon task performance we would expect to see reduced correlation against the $n = 12$ targets in the Full feedback condition. For APB–ADM, correlation between Full feedback hold score and Reach and Zero feedback scores were both significant: ($r = 0.98, n = 12, p <$

10^{-4}) and ($r = 0.89, n = 12, p < 10^{-3}$), respectively. The same conditions were also significant for FCR–ECR: ($r = 0.99, n = 12, p < 10^{-4}$) and ($r = 0.81, n = 12, p < 10^{-2}$). In the case of 1DI–APB correlation between Full feedback and Reach feedback hold score was significant ($r = 0.90, n = 12, p < 10^{-4}$) but correlation between Full feedback and Zero feedback failed to reach significance ($r = 0.53, n = 12, p = 0.08$). Correlation between Full feedback hold scores and Reach feedback hold scores were significantly higher in both APB–ADM and FCR–ECR than 1DI–APB, (Raghunathan's z-test, $Z = 2.24, p = 0.025$), with the same significance values in both cases. This may be explained by the fact that participants rely upon visual feedback to recognise and to react to undesirable co-activation; when feedback is not available during the hold period participants were less able to ameliorate co-activation.

3.2. Performance improvement, learning and generalisation

Improvement in performance over runs and the relationship between these performance gains and feedback across each muscle pair are summarised in figure 5. Figure 5(a) shows increase in hold score for each muscle pair *relative* to participant performance on their initial run in the Full feedback condition. No significant differences were found between improvement rates in the two intrinsic muscle groups. Significant differences were found in rates of improvement, i.e. over the resulting $n = 7$ increments, between APB–ADM ($Mdn = 0.23$) and FCR–ECR ($Mdn = 0.18$) (Wilcoxon Signed-Ranks Test, $p = 0.015$) and 1DI–APB ($Mdn = 0.22$) and FCR–ECR ($Mdn = 0.18$) (Wilcoxon Signed-Ranks Test, $p = 0.01$). Neither of the intrinsic muscle pairs show any sign of plateauing. In contrast improvement rates for FCR–ECR levelled out in the final experimental runs.

The degree to which performance in the Full feedback condition generalises across the reduced feedback conditions is summarised in figure 5(b). In the case of Reach feedback, a close to linear relationship exists between performance rates and those found in the Full feedback condition: APB–ADM ($r = 0.97, n = 8, p < 10^{-4}$), 1DI–APB ($r = 0.99, n = 8, p < 10^{-4}$) and FCR–ECR ($r = 0.99, n = 8, p < 10^{-4}$). In the case of APB–ADM, a similar relationship exists between the Full feedback and the Zero feedback conditions ($r = 0.92, n = 8, p < 0.005$). Relative to the Reach condition, reduced strength relationships exist between performance in the Full feedback and the Zero feedback conditions for both 1DI–APB ($r = 0.86, n = 8, p < 10^{-2}$) (Meng's z-test, $Z = 3.04, p < 10^{-2}$), and FCR–ECR ($r = 0.70, n = 8, p = 0.055$) (Meng's z-test, $Z = 3.5$, $p < 10^{-3}$).

3.3. Effect of feedback on performance

The main effects of feedback condition on MCI performance are summarised in figure 6. Overall hold scores for individual participants in each of the three feedback conditions, with participants ordered according to their hold scores in the Full feedback condition, are shown in figure 6(a). Participants performance using Full feedback predicts performance in the alternative conditions, correlating strongly with both the Reach ($r = 0.97, n = 24, p < 10^{-3}$) and Zero feedback condition ($r = 0.90, n = 24, p < 10^{-3}$). As outlined in figure 6(b), significant differences were found when comparing median hold score in the Zero feedback condition ($Mdn = 0.24$) against both the Full ($Mdn = 0.5$): (Wilcoxon Signed-Ranks Test, $Z = 4.96, p < 10^{-3}$) and Reach ($Mdn = 0.48$): (Wilcoxon Signed-Ranks Test, $Z = 4.44, p < 10^{-3}$), feedback conditions. A significantly reduced hold score in the Zero feedback condition may be attributable either to participants failing to reach the target, or to participants failing to maintain the cursor within the target. We measure ability to reach

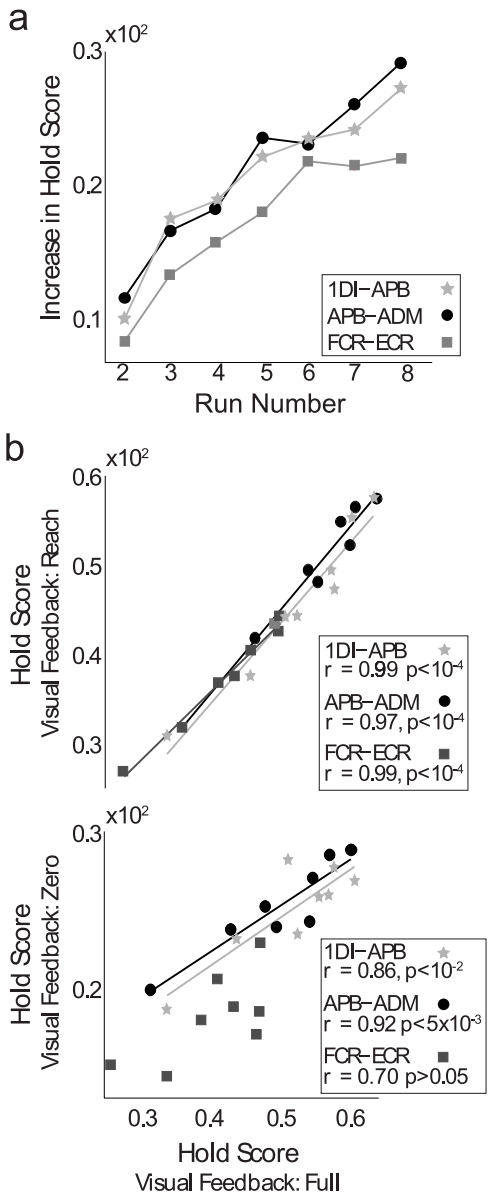

Figure 5. Performance improvement over runs and feedback conditions. (a) Increase in hold score relative to the initial run in the Full feedback condition. (b) Relationship between performance in the Full feedback condition and that in the Reach and Zero feedback conditions. Lines of best fit indicate significant correlation in performance across feedback conditions.

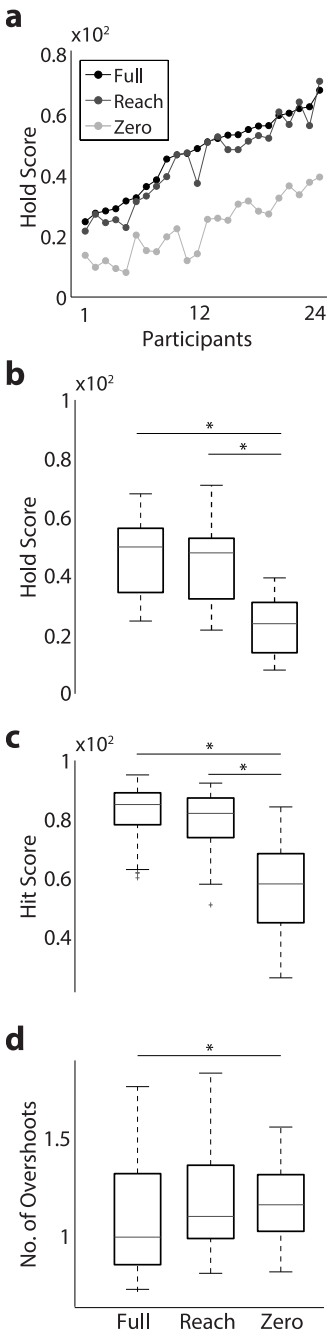

Figure 6. Salient relationships between feedback conditions. (a) Individual participant scores for the three feedback conditions, ordered according to their performance in the Full feedback condition. (b)–(d) Box plots outline differences between feedback conditions; (b) Hold score (c) Hit score and (d) Number of overshoots. Asterisks denote statistical significance and the + sign symbolises an outlier.

targets using hit score. The same pattern of differences is observed in figure 6(c) which shows significant differences in hit score in the Zero feedback condition ($Mdn = 0.58$) in comparison to the both the Full ($Mdn = 0.85$): (Wilcoxon Signed-Ranks Test, $Z = 4.94, p < 10^{-3}$) and Reach ($Mdn = 0.82$): (Wilcoxon Signed-Ranks Test, $Z = 4.66, p < 10^{-3}$), feedback conditions. Failure to maintain the cursor in contact with the target would lead to an increased number of overshoots. Figure 6(d) shows the number of overshoots during the hold period across feedback conditions. A Wilcoxon Signed-Ranks Test indicated that the median number of overshoots in the Full feedback condition ($Mdn = 0.99$) was significantly lower than the number of overshoots in the Zero feedback condition ($Mdn = 1.15$) ($Z = -2.24, p < 0.05$). No condition differed significantly in terms of overshoots against the Reach feedback condition.

3.4. Relationship between performance and motor variability

A number of salient measures were obtained and analysed to determine which best account for improvement in participant scores with training. Increased MCI performance was generally observed to be negatively correlated to participant reaction time, overall cursor speed and the time taken for the cursor to reach each individual targets. Path efficiency, the optimal trajectory from origin to target over the actual trajectory taken, was positively correlated with MCI performance. Full details of descriptive statistics may be found in supplementary materials in table S1.

Coefficient of variation (CV) was the most consistently predictive metric both within and across participants. A relationship between CV and hold score could be predicted from the behaviour expected, but not strictly necessary, to complete the MCI task. That is to say, the most efficient method of performing the task is to generate, and rely upon reproducing, internal representations of the levels of muscle activity required to reach targets. Following, EMG would become more consistent over time, reducing its CV, as participants continually refine internal models of the required activity. In this context, CV can be interpreted either as measuring a biological mechanism, in the form of motor noise [60], or behavioural adaptation, as participant strategy moves from reactive feedback led activity to proactive use of internal models. Because CV is sensitive both to stochastic noise and to fluctuations in the EMG signal, differentiation between these competing hypotheses is challenging. Irrespective, in the context of myoelectric control, the CV measure provides information over and above that contained in the MAV measure.

3.4.1. General overview. Figure 7 summarises the high level relationships found between CV, hold score and muscle control pairs. Viewed across participants ($n = 24$ participants) with data amalgamated over runs, a significant negative correlation was found between hold score and CV for muscle group APB–ADM ($r = -0.58, n = 24, p < 10^{-2}$) as shown in figure 7(a), and 1DI–APB ($r = -0.45, n = 24, p = 0.024$), demonstrating that participants with lower overall CV trended toward better hold scores. No significant relationship was found for the FCR–ECR pairing. Similarly, changes in CV over runs were also predictive of improvements in performance. With data amalgamated across participants and viewed across runs ($n = 8$ runs), strong correlations were found between hold score and CV in all muscle groups, APB–ADM ($r = -0.98, n = 8, p < 10^{-4}$), 1DI–APB ($r = -0.95, n = 8, p < 10^{-2}$) and FCR–ECR ($r = -0.96, n = 8, p < 10^{-4}$).

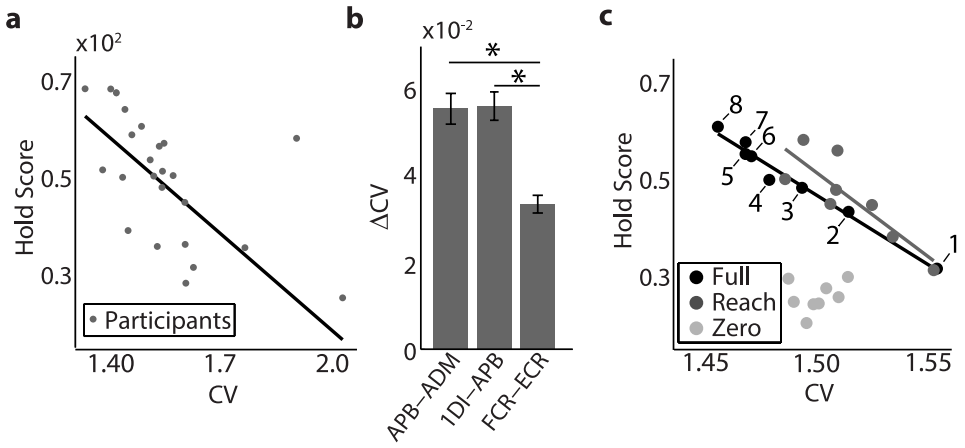

Figure 7. Coefficient of variation as an alternative measure. (a) Relationship between individual participant's EMG coefficient of variation (CV) and their hold score in the Full feedback condition for the APB–ADM pair. (b) Absolute change as ΔCV between the first and final runs for each muscle group. Asterisks show significance. (c) Relationship between average CV and hold score over runs for muscle pair APB–ADM. Lines of best fit are included where correlation is significant. Run numbers are labelled in the Full feedback condition.

Significant negative correlation between CV and MCI performance necessitates a quantifiable reduction in CV over runs. To quantify the degree to which CV changes across muscle pairs, we compared the absolute change in coefficient of variation over the experimental period, expressed as the delta between CV in the final run relative to that in the first run, across participants. The absolute change in coefficient of variation over runs is shown in figure 7(b). The magnitude of change in CV for FCR–ECR ($Mdn = 0.03$) was significantly smaller than both APB–ADM ($Mdn = 0.05$) (Wilcoxon Signed-Ranks Test, $Z = 3.83, p < 10^{-3}$) and 1DI–APB ($Mdn = 0.06$) (Wilcoxon Signed-Ranks Test, $Z = 4.11, p < 10^{-4}$). These changes mirror the performance differences presented in figure 3(a). A reduced range of change for the FCR–ECR pair may indicate a reduced ability to modulate motor noise or a more limited capacity for reactive, feedback led, behaviour.

3.4.2. Influence of visual feedback. To determine whether visual feedback played a role in reducing the variability of the EMG signals, we compared the relationship between CV and MCI performance in the Reach and Zero feedback trials to that in the Full feedback condition. Permutation distributions of correlation values were generated by re-sampling Full feedback trials using trial counts equivalent to catch conditions, amalgamating data across participants and then correlating over runs ($n = 8$ runs).

The average CV values and hold scores obtained from repeated re-sampling of Full feedback trials for muscle pair APB–ADM are shown, along with Reach and Zero feedback trial data, in figure 7(c). When comparing permutation distributions, no significant differences were observed in the degree of correlation between hold score and CV in the Full feedback and the Reach feedback conditions for APB–ADM and 1DI–APB. In the case of FCR–ECR, while the hold score for Full and Reach feedback were in a similar range, the CV for Reach feedback was more compressed than that of the Full feedback condition, leading to a significant reduction in correlation (permutation test, $n = 8, p < 10^{-2}$). This observation suggests that visual feedback may play a greater role in reducing the variability of the EMG signals in the extrinsic muscles, however this does not significantly impact upon hold score.

3.4.3. Temporal changes in performance. A limited influence of visual feedback suggests a feed-forward approach reduces the variability of the EMG signals. We therefore extended our analysis to include the reach period to determine whether a reduced variability in the EMG signals, earlier in the trial period, predicted enhanced performance. Time series CV values were generated by calculating windowed CV over 100 ms periods, incrementing in steps of 5 ms. The CV time series data were amalgamated across participants and viewed across runs. For each 5 ms time step, we obtained the Pearson's linear coefficient (ρ) and significance level associated with correlating windowed CV and performance. This produced the time series in figure 8(a) that describes the strength and significance of the relationship over the course of the trial period, extending figure 7(c).

The time series for the ρ of muscle pair APB–ADM, CV against hold score is shown in figure 8(a). Shading in this figure indicates uncorrected significance at the 0.01 level. Lower levels of motor variability early in the trial period; 470 ms for APB–ADM, from around 400 ms for 1DI–APB and from 550 ms for FCR–ECR; were significantly related to participant performance as measured by hold score. This indicates that enhanced MCI task performance is associated with participants producing consistent low variability muscle activity from as early as 300 ms after target presentation. The time series CV and its standard error, for muscle pair APB-ADM are shown in the upper part of figure 8(b) for the first and final experimental runs. It may be observed that CV drops earlier and more rapidly in later trials and rests at a lower level during the hold period. The lower part of figure 8(b) shows equivalent MAV values. In early trials MAV peaks somewhere in the region of 900 ms after target presentation. In late trials MAV peaks approximately 500 ms after the target is presented. The

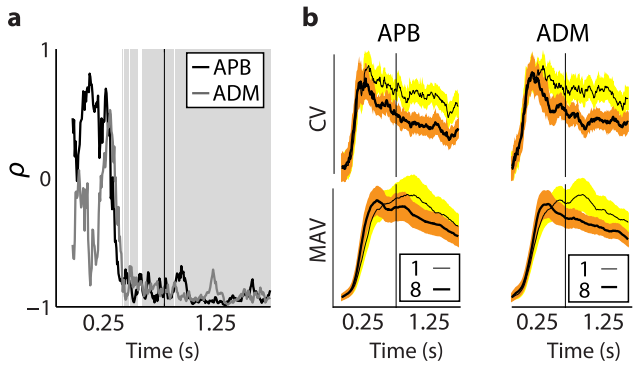

Figure 8. Changes in coefficient of variation within a trial. Sample data from muscle pair APB–ADM. (a) Pearson's ρ between windowed CV and hold score over the trial period ($n = 8$). Shaded periods indicate where correlation between CV and hold score are significant at the 0.01 level (uncorrected). (b) Windowed CV and equivalent MAV of EMG and their standard error over the trial period. Graphs are shown for the first and final runs.

trend of earlier MAV peaks occurs across all muscles groups, suggesting participants learn to buffer high magnitude muscle activity into the earlier parts of the trial period.

4. Discussion

4.1. Overall MCI performance

The intrinsic muscle groups tested outperformed extrinsic muscles in control of an abstract decoder. Within the intrinsic pairs, we observed no significant differences in performance between use of an independent muscle pair and use of a synergist pair. This observation corroborates earlier work confirming that intrinsic hand muscles can form new task-specific functional muscle synergies to meet task requirements [15, 16, 18, 21].

Within each muscle group a spatial pattern of performance, in the task space, exists whereby higher scores are obtained for peripheral 'edge column' targets than targets in the central columns. This is consistent with predictions of signal dependent noise when multiple effectors control current state [61]. Although it may be assumed that this shape is generated due to initially poor performance using paired muscles relative individual ones, we observe similar patterns in later runs due to relatively uniform improvement in ability across targets. Within central targets, we additionally observe a more pronounced performance drop with progressing rows, again consistent with predictions of signal-dependent noise as increased magnitude of activity implies increased variability. Single trial cursor trajectories and the spatial performance map for the synergist pair, 1DI–APB, indicate muscle co-activation as evidenced in reduced hold scores across the upper right targets.

The implications of signal-dependent noise on prosthesis control are well understood and the effects may be mitigated by ensuring neighbouring functional outputs share a degree of similarity rather than opposing functions. While in this study, we observe poorer performance for central column targets, these effects are likely reduced with continual practice. Co-activation is possibly more relevant in this context as it suggests some users may have difficulty completely dissociating existing synergist muscle pairs, even at low levels of muscle activation. Interestingly, we observed that participants only appeared to be aware of this co-activation during the visual feedback condition which would not necessarily be available during prosthesis use.

4.2. Performance improvement, learning and generalisation

Learning effects were observed across each muscle group. Data presented in section 3.2 supports an early exploratory period, during which it is likely that participants rely upon continuous feedback to generate inverse maps [27]. This exploratory period is particularly evident in early improvements in hit score, as shown in figure S2 in supplementary materials. The gains in cursor control which increase hit score are a prerequisite for improved hold score, as shown in figure S3 in supplementary materials. Learning rates, as measured by participants improvement over runs, were significantly higher for the intrinsic muscle pairs than the extrinsic muscle pair. This relationship between distal and proximal muscles is consistent with observations in [20]. Of equal significance, the manner in which gains generalise between feedback conditions also differs when comparing the intrinsic and extrinsic muscle groups. While each muscle pair generalised in a similar manner to the Reach feedback condition, only the intrinsic muscle pairs showed a consistent transfer of learning to the Zero feedback condition.

Differences in rates of learning, and in the manner in which learning is internalised, suggest that intrinsic muscle groups have the capability to unlock the full potential of modern multi-functional myoelectric prostheses, namely the proportional myoelectric control [21] of multiple grip patterns [24]. While this may have been immaterial in the recent past, the advent of digit prostheses for partial-hand loss now demands new control strategies based on intrinsic muscles be properly explored. Two factors impede the degree of functionality which may be achieved through myoelectric control based on intrinsic hand muscles; the physical structure of the hand, and the neural substrates which underlie its control. After digit loss, many of the anatomical constraints which normally limit the independence of intrinsic muscles are removed. Although we found evidence of existing hand synergies affecting performance, these effects are limited, consistent with the adaptation of synergies toward new task-specific roles [15, 16, 18, 21]. We believe that judicious consideration of these factors will open up the possibility of fully flexible neural control. Further experiments with amputee populations are required to test these hypotheses.

4.3. Effect of feedback on performance

The data presented in section 3.3 demonstrates that visual feedback is used to guide movement of the cursor to the target. However, feedback is not necessary in maintaining cursor position once the target has been reached. Participants produce

a higher median number of overshoots in the Zero feedback condition, with a reduced upper bound. This distribution is likely to represent the cursor regularly passing through the target in the Zero feedback condition. Passing through the target would be congruent with the notion that feedback is used to ascertain the current state, rather than to maintain it.

Afferents of muscle spindles provide information normally used to sense movement and position [62] and may be used in the absence of vision [63]. Earlier studies with similar myoelectric-controlled interfaces showed that mechanical [20] and electrical [18] perturbations of the proprioceptive feedback from the controlling muscles do not reveal any major role for proprioception; likely because movements performed by participants were near-isometric. However, in the task space that was proposed in this paper, it is possible that feedback from receptors sensitive to muscle tension, i.e. the golgi tendon organs, is used to maintain stable contraction levels. The use of this type of proprioceptive feedback would also be congruent with the notion that, upon learning, a mapping is developed between the task space and relative muscle tension, potentially allowing participants to reach the target without visual aid. Further control experiments may be needed to verify this hypothesis.

The results in the Zero feedback condition do not preclude real-world use of an abstract decoder with a prosthesis. As outlined in figure 6(a), each participant's performance in the Zero feedback condition parallels their ability in the Full and Reach conditions. We anticipate that real use of these methods may utilise the economic feedback protocol hypothesized by Dosen *et al* to gradually reduce overall reliance on feedback whilst also providing intermittent information to ensure internal models remain stable [64]. It may be the case that other forms of feedback, such as artificial proprioception [23], vibro-tactile stimulation [65], or audio augmented feedback [66] will be more appropriate to provide information about the current state, in order to facilitate the development of the internal model.

4.4. Relationship between performance and motor variability

A number of metrics were observed to be correlated to participants' performance which, as an ensemble, outline general motor learning. We observed a reduction in reaction time, commonly associated with motor skill acquisition [67], along with a reduction in overall cursor speed, likely to be a consequence of increased control and a reduction in the frequency of ballistic movements. Control gains were also apparent in improved cursor path efficiency which, along with faster reaction times, contribute to significant reductions in the time taken to reach individual targets.

The most predictive measure of performance was the variability of the EMG signals, typically interpreted as the physical embodiment of noise generated within the sensorimotor process [68–70]. Motor control theories propose that the impact of noise on task performance is actively curtailed during motor planning [61, 71, 72] or minimised in conjunction with effort [73–75]; however recent research also suggests motor variability is actively regulated to facilitate learning [76]. Reduction in variability could therefore be explained by enhanced motor control or as a shift away from exploration of the task space. In the case of task space exploration, the dexterity of intrinsic muscles may explain the enhanced range of CV observed. As discussed earlier, because our measure of variability is sensitive both to stochastic noise and to EMG fluctuations associated with exploratory learning, we cannot dissociate these competing hypothesis.

During initial MCI use, participants are particularly reliant upon visual feedback to reach targets, but can maintain cursor position irrespective of feedback condition. Similarly, overall relations between hold period motor noise and MCI performance are invariant to feedback condition. Enhanced task performance was related to participants ability to perform consistent EMG activations very quickly after target presentation, a behaviour which was paralleled by changes in the MAV profile used to reach targets, as shown in figure 8(b). The skewed MAV profile observed in late trials is contingent with minimum-variance models which optimise performance by producing larger commands earlier, allowing for more time to detect and correct any errors resulting from control-dependent noise [74]. These analyses indicate an internally driven, feed-forward, process acts to reduce motor variability, in line with typical motor skill acquisition.

It is likely that coefficient of variation provides a more nuanced measure of the quality of control than the hold score measure. This would explain why correlation data for motor noise were highly consistent, both within and across participants and runs. We are investigating to what degree coefficient of variation can be utilised as a proxy for confidence in user output in a prosthetic decoding context.

4.5. Implications for myoelectric prosthesis control

A growing body of research suggests abstract decoding is the most prudent control strategy for upper-limb prosthesis when using intrinsic muscle groups and the approach has generated commercial interest [77]. In addition, academic research shows that alternative approaches for partial-hand control are necessary, because intrinsic sites alone are currently insufficient to determine grasp using pattern recognition [78]. The differences in performance and rates of learning presented in this work do not preclude abstract decoding using extrinsic muscles [24, 33]. Relative to intrinsic control, proficient extrinsic control takes longer to master and is typically less refined during early decoder use. Longer, and often unpredictable, training times make it more difficult to assess abstract decoding based on extrinsic muscles and could limit the approach. In users with limb loss, the effects of muscle atrophy on stamina can also reduce the feasible duration of training sessions. The data presented in this paper cannot address these issues. We are therefore performing real-time experiments to test the efficacy of the MCI task presented with a cohort of people with limb difference. This small scale clinical trial is conducted with approval from the UK National Health Service (NHS) [79]. Preliminary results demonstrate

that with a more structured training approach control can be achieved both by individuals with trans-radial limb loss and also those with trans-humeral loss [80].

Of perhaps more importance, the shown differences across muscle groups mean that research on trans-radial amputees cannot be extrapolated to the partial-hand population. Differences in intrinsic and extrinsic musculature are likely to alter the degree to which prosthesis users value intuitive control. In the case of trans-radial amputees, use of pattern recognition provides both more intuitive control and a greater number of DoFs than traditional dual-site control [81]. In contrast, our results suggest that by forfeiting intuitive control, intrinsic muscles can rapidly learn control of several DoF.

In conclusion, pattern recognition relies upon the use of pre-existing inverse maps and pre-existing patterns of muscle activity to form reference points, classes, via which a user and a device can communicate. This type of communication may be intuitive but its bandwidth is typically limited. The physiology of the hand provides the capacity to quickly develop novel inverse maps and the ability to rapidly couple and decouple muscles to form task-dependent functional groups. Both of these factors, along with increased fractionation of muscle activity, suggest that motor learning based approaches will provide more enhanced control in the case of partial-hand prostheses.

Acknowledgments

The authors thank Prof Kevin Englehart of the University of New Brunswick for many helpful comments on an earlier version of this paper. This work is supported by the UK Engineering and Physical Sciences Research Council (EPSRC) research grant EP/M025594/1.

Open access statement

Data supporting this publication is openly available under an 'Open Data Commons Open Database License'. Additional metadata are available at: https://doi.org/10.17634/137930-4.

ORCID iDs

Matthew Dyson https://orcid.org/0000-0002-8707-0137
KianoushNazarpour https://orcid.org/0000-0003-4217-0254

References

[1] Parker P, Englehart K B and Hudgins B 2006 Myoelectric signal processing for control of powered limb prostheses *J. Electromyogr. Kinesiol.* **16** 541–8
[2] Kuiken T, Dumanian G, Lipschutz R, Miller L and Stubblefield K 2004 The use of targeted muscle reinnervation for improved myoelectric prosthesis control in a bilateral shoulder disarticulation amputee *Prosthet. Orthot. Int.* **28** 245–53
[3] Kuiken T, Li G, Lock B, Lipschutz R, Miller L, Stubblefield K and Englehart K 2009 Targeted muscle reinnervation for real-time myoelectric control of multifunction artificial arms *J. Am. Med. Assoc.* **301** 619–28
[4] Hargrove L J, Miller L A, Turner K and Kuiken T A 2017 Myoelectric pattern recognition outperforms direct control for transhumeral amputees with targeted muscle reinnervation: a randomized clinical trial *Sci. Rep.* **7** 13840
[5] Uellendahl J and Uellendahl E 2012 Experience fitting partial hand prostheses with externally powered fingers *Grasping the Future: Advances in Powered Upper Limb Prosthetics* ed V P Castelli and M Troncossi (Sharjah: Bentham Books) ch 3, pp 15–27
[6] Ziegler-Graham K, MacKenzie E, Ephraim P, Travison T and Brookmeyer R 2008 Estimating the prevalence of limb loss in the United States: 2005–2050 *Arch. Phys. Med. Rehabil.* **89** 422–9
[7] United National Institute for Prosthetics and Orthotics Development (UNIPOD) 2013 Limbless statistics (formerly national amputee statistical database [nasdab] annual report 2010-2011) www.limbless-statistics.org [Online; accessed 7-March-2017]
[8] Davidson J 2004 A comparison of upper limb amputees and patients with upper limb injuries using the disability of the arm, shoulder and hand (DASH) *Disability Rehabil.* **26** 917–23
[9] Burger H, Maver T and Marincek C 2007 Partial hand amputation and work *Disability Rehabil.* **29** 1317–21
[10] Lang M 2011 Challenges and solutions in control systems for electrically powered articulating digits *MEC Symp. Conf. Proc.* (UNB)
[11] Zinck A, Kyberd P, Hill W, Bush G, Stavdahl O, Biden E and Fraser K 2008 A study of the use of compensation motions when using prosthetic wrists *MEC Symp. Conf. Proc.* (UNB)
[12] Bertels T, Schmalz T and Ludwigs E 2009 Objectifying the functional advantages of prosthetic wrist flexion *J. Prosthet. Orthot.* **21** 74–8
[13] Lemon R N 1993 The G. L. Brown prize lecture. cortical control of the primate hand *Exp. Physiol.* **78** 263–301
[14] Lemon R N 2008 Descending pathways in motor control *Ann. Rev. Neurosci.* **31** 195–218
[15] Lang C and Schieber M H 2004 Human finger independence: limitations due to passive mechanical coupling versus active neuromuscular control *J. Neurophysiol.* **92** 2802–10
[16] Ison M and Artemiadis P 2014 The role of muscle synergies in myoelectric control: trends and challenges for simultaneous multifunction control *J. Neural Eng.* **11** 051001
[17] de Rugy A, Loeb G E and Carroll T J 2012 Muscle coordination is habitual rather than optimal *J. Neurosci.* **32** 7384–91
[18] Nazarpour K, Barnard A and Jackson A 2012 Flexible cortical control of task-specific muscle synergies *J. Neurosci.* **32** 12349–60
[19] Ison M and Artemiadis P 2015 Proportional myoelectric control of robots: muscle synergy development drives performance enhancement, retainment, and generalization *IEEE Trans. Robot.* **31** 259–68
[20] Radhakrishnan S M, Baker S N and Jackson A 2008 Learning a novel myoelectric-controlled interface task *J. Neurophysiol.* **100** 2397–408
[21] Pistohl T, Cipriani C, Jackson A and Nazarpour K 2013 Abstract and proportional myoelectric control for multi-fingered hand prostheses *Ann. Biomed. Eng.* **41** 2687–98
[22] Antuvan C W, Ison M and Artemiadis P 2014 Embedded human control of robots using myoelectric interfaces *IEEE Trans. Neural Syst. Rehabil. Eng.* **22** 820–7

[23] Pistohl T, Josh D, Ganesh G, Jackson A and Nazarpour K 2015 Artificial proprioceptive feedback for myoelectric control *IEEE Trans. Neural Syst. Rehabil. Eng.* **23** 498–507
[24] Segil J L and Weir R F 2015 Novel postural control algorithm for control of multifunctional myoelectric prosthetic hands *J. Rehabil. Res. Dev.* **52** 449–66
[25] Wolpert D M and Kawato M 1998 Multiple paired forward and inverse models for motor control *Neural Netw.* **11** 1317–29
[26] Mussa-Ivaldi F A, Casadio M, Danziger Z C, Mosier K M and Scheidt R A 2011 Sensory motor remapping of space in human-machine interfaces *Prog. Brain Res.* **191** 45–64
[27] Liu X and Scheidt R A 2008 Contributions of online visual feedback to the learning and generalization of novel finger coordination patterns *J. Neurophysiol.* **99** 2546–57
[28] Liu X, Mosier K M, Mussa-Ivaldi F A, Casadio M and Scheidt R 2011 Reorganization of finger coordination patterns during adaptation to rotation and scaling of a newly learned sensorimotor transformation *J. Neurophysiol.* **105** 454–73
[29] Héliot R, Ganguly K, Jimenez J and Carmena J 2010 Learning in closed-loop brain-machine interfaces: modeling and experimental validation *IEEE Trans. Syst. Man Cybern.* B **40** 1387–97
[30] Mosier K M, Scheidt R A, Acosta S and Mussa-Ivaldi F A 2005 Remapping hand movements in a novel geometrical environment *J. Neurophysiol.* **94** 4362–72
[31] Wright Z A, Zev Rymer W and Slutzky M W 2014 Reducing abnormal muscle co-activation after stroke using a myoelectric-computer interface: a pilot study *Neurorehabilitation Neural Repair* **28** 443–51
[32] Nazarpour K, Cipriani C, Farina D and Kuiken T 2014 Guest editorial: advances in control of multi-functional powered upper-limb prostheses *IEEE Trans. Neural Syst. Rehabil. Eng.* **22** 711–5
[33] Hahne J M, Markovic M and Farina D 2017 User adaptation in myoelectric man-machine interfaces *Sci. Rep.* **7** 4437
[34] Cipriani C, Antfolk C, Controzzi M, Lundborg G, Rosén B, Carrozza M C and Sebelius F 2011 Online myoelectric control of a dexterous hand prosthesis by transradial amputees *IEEE Trans. Neural Syst. Rehabil. Eng.* **19** 260–70
[35] Ngeo J G, Tamei T and Shibata T 2014 Continuous and simultaneous estimation of finger kinematics using inputs from an EMG-to-muscle activation model *J. NeuroEng. Rehabil.* **11** 122
[36] Hahne J M, Biebmann F, Jiang N, Rehbaum H, Farina D, Meinecke F C, Muller K R and Parra L C 2014 Linear and nonlinear regression techniques for simultaneous and proportional myoelectric control *IEEE Trans. Neural Syst. Rehabil. Eng.* **22** 269–79
[37] Krasoulis A, Vijayakumar S and Nazarpour K 2015 Evaluation of regression methods for the continuous decoding of finger movement from surface EMG and accelerometry *7th Int. IEEE/EMBS Conf. on Neural Engineering* (NER) pp 631–4
[38] Clancy E A, Martinez-Luna C, Wartenberg M, Dai C and Farrell T R 2017 Two degrees of freedom quasi-static EMG-force at the wrist using a minimum number of electrodes *J. Electromyogr. Kinesiol.* **34** 24–36
[39] Cipriani C, Segil J L, Birdwell J A and ff Weir R F 2014 Dexterous control of a prosthetic hand using fine-wire intramuscular electrodes in targeted extrinsic muscles *IEEE Trans. Neural Syst. Rehabil. Eng.* **22** 828–36
[40] Smith L H, Kuiken T A and Hargrove L J 2014 Real-time simultaneous and proportional myoelectric control using intramuscular EMG *J. Neural Eng.* **11** 066013
[41] Smith L H, Kuiken T A and Hargrove L J 2015 Use of probabilistic weights to enhance linear regression myoelectric control *J. Neural Eng.* **12** 066030
[42] Hudgins B, Parker P and Scott R N 1993 A new strategy for multifunction myoelectric control *IEEE Trans. Biomed. Eng.* **40** 82–94
[43] Englehart K and Hudgins B 2003 A robust, real-time control scheme for multifunction myoelectric control *IEEE Trans. Biomed. Eng.* **50** 848–54
[44] Fetz E E 1969 Operant conditioning of cortical unit activity *Science* **163** 955–8
[45] Taylor D M, Helms Tillery S I and Schwartz A B 2002 Direct cortical control of 3D neuroprosthetic devices *Science* **296** 1829–32
[46] Mortiz C T, Perlmutter S I and Fetz E E 2008 Direct control of paralysed muscles by cortical neurons *Nature* **456** 639–42
[47] Ganguly K and Carmena J M 2009 Emergence of a stable cortical map for neuroprosthetic control *PLOS Biol.* **7** e1000153
[48] Ganguly K, Dimitrov D F, Wallis J D and Carmena J M 2011 Reversible large-scale modification of cortical networks during neuroprosthetic control *Nat. Neurosci.* **14** 662–7
[49] Law A J, Rivlis G and Schieber M H 2014 Rapid acquisition of novel interface control by small ensembles of arbitrarily selected primary motor cortex neurons *J. Neurophysiol.* **112** 1528–48
[50] Jarosiewicz B, Chase S M, Fraser G W, Velliste M, Kass R E and Schwartz A B 2008 Functional network reorganization during learning in a brain computer interface paradigm *Proc. Natl Acad. Sci. USA* **105** 19486–91
[51] Sadtler P T, Quick K M, Golub M D, Chase S M, Ryu S I, Tyler-Kabara E C, Yu B M and Batista A P 2014 Neural constraints on learning *Nature* **512** 423–6
[52] Hall T M, Nazarpour K and Jackson A 2014 Real-time estimation and biofeedback of single-neuron firing rates using local field potentials *Nat. Commun.* **5** 5462
[53] Graziadio S, Nazarpour K, Gretenkord S, Jackson A and Eyre J 2015 Greater intermanual transfer of feed forward learning in the elderly: evidence that age related bilateral motor cortex activation is compensatory *J. Motor Behav.* **47** 47–55
[54] Ghazaei G, Alameer A, Degenaar P, Morgan G and Nazarpour K 2017 Deep learning-based artificial vision for grasp classification in myoelectric hands *J. Neural Eng.* **14** 036025
[55] Lake C 2009 Experience with electric prostheses for the partial hand presentation: and eight-year retrospective *J. Prosthet. Orthot.* **21** 125–30
[56] Solnik S, DeVita P, Rider P, Long B and Hortobágyi T 2008 Teager–Kaiser operator improves the accuracy of EMG onset detection independent of signal-to-noise ratio *Acta Bioeng. Biomech.* **10** 65–8
[57] Solnik S, Rider P, Steinweg K, DeVita P and Hortobágyi T 2010 Teager–Kaiser energy operator signal conditioning improves EMG onset detection *Eur. J. Appl. Physiol.* **110** 489–98
[58] Li X and Aruin A 2005 Muscle activity onset time detection using Teager–Kaiser energy operator *Proc. IEEE Engineering in Medicine and Biology Annual Conf.*
[59] Diedenhofen B and Musch J 2015 cocor: a comprehensive solution for the statistical comparison of correlations *PLOS One* **10** e0121945
[60] Hamilton A F, Jones K E and Wolpert D M 2004 The scaling of motor noise with muscle strength and motor unit number in humans *Exp. Brain Res.* **157** 417–30
[61] Harris C M and Wolpert D M 1998 Signal-dependent noise determines motor planning *Nature* **394** 780–4
[62] Clark F J, Burgess R C, Chapin J W and Lipscomb W T 1985 Role of intramuscular receptors in the awareness of limb position *J. Neurophysiol.* **54** 1529–40
[63] Goodwin G M, McCloskey D I and Matthews P B C 1972 The contribution of muscle afferents to kinaesthesia shown by

vibration induced illusions of movement and by the effects of paralysing the joint afferents *Brain* **95** 705–48
[64] Dosen S, Markovic M, Wille N, Henkel M, Koppe M, Ninu A, Frömmel C and Farina D 2015 Building an internal model of a myoelectric prosthesis via closed-loop control for consistent and routine grasping *Exp. Brain Res.* **233** 1855–65
[65] Witteveen H J B, Luft F, Rietman J S and Veltink P H 2014 Stiffness feedback for myoelectric forearm prostheses using vibrotactile stimulation *IEEE Trans. Neural Syst. Rehabil. Eng.* **22** 53–61
[66] Shehata A W, Scheme E J and Sensinger J W 2018 Myoelectric prosthesis control: improving internal model strength and performance using augmented feedback (bioRxiv:259754) https://doi.org/10.1101/259754
[67] Singer R N 1980 *Motor Learning and Human Performance: an Application to Motor Skills and Movement Behaviors* 3rd edn (London: Macmillan)
[68] Schmidt R A, Zelaznik H, Hawkins B, Frank J Sand Quinn J T Jr 1979 Motor-output variability: A theory for the accuracy of rapid motor acts *Psychol. Rev.* **86** 415–51
[69] Jones K E, Hamilton A F and Wolpert D M 2002 Sources of signal-dependent noise during isometric force production *J. Neurophysiol.* **88** 1533–44
[70] Stein R B, Gossen E R and Jones K E 2005 Neuronal variability: noise or part of the signal *Nat. Rev. Neurosci.* **6** 389–97
[71] Scholz J P and Schöner G 1999 The uncontrolled manifold concept: identifying control variables for a functional task *Exp. Brain Res.* **126** 289–306
[72] van Beers R J, Baraduc P and Wolpert D M 2002 Role of uncertainty in sensorimotor control *Phil. Trans. R. Soc.* **357** 1137–45
[73] Todorov E and Jordan M I 2002 Optimal feedback control as a theory of motor coordination *Nat. Neurosci.* **5** 1226–35
[74] Todorov E 2004 Optimality principles in sensorimotor control *Nat. Neurosci.* **7** 907–15
[75] O'Sullivan I, Burdet E and Diedrichsen J 2009 Dissociating variability and effort as determinants of coordination *PLoS Comput. Biol.* **5** e1000345
[76] Wu H G, Miyamoto Y R, Nicolas Gonzalez Castro L, Ölveczky B P and Smith M A 2014 Temporal structure of motor variability is dynamically regulated and predicts motor learning ability *Nat. Neurosci.* **17** 312–21
[77] Meijer R and Nazarpour K 2015 *US Patent Specification* US20150374515A1 (https://patents.google.com/patent/US20150374515A1)
[78] Adewuyi A A, Hargrove L J and Kuiken T A 2016 An analysis of intrinsic and extrinsic hand muscle EMG for improved pattern recognition control *IEEE Trans. Neural Syst. Rehabil. Eng.* **24** 485–94
[79] Jones H and Nazarpour K 2018 Gaining NHS ethical approval from the perspective of a biomedical engineering team *Br. J. Healthc. Manag.* **24** 71–6
[80] Dyson M and Nazarpour K 2018 Data driven spatial filtering can enhance abstract myoelectric control in amputees *40th Int. IEEE/EMBS Conf. (EMBC)*
[81] Young A J, Smith L H, Rouse E J and Hargrove L J 2013 Classification of simultaneous movements using surface EMG pattern recognition *IEEE Trans. Biomed. Eng.* **60** 1250–8